VIII International Conference on Computational Plasticity
COMPLAS VIII
E. Oñate and D.R.J. Owen (Eds)
©CIMNE, Barcelona, 2005

ENERGY-DISSIPATIVE MOMENTUM-CONSERVING TIME-STEPPING ALGORITHMS FOR DYNAMIC FINITE STRAIN PLASTICITY

Francisco Armero

Department of Civil and Environmental Engineering
University of California at Berkeley
713 Davis Hall, Berkeley CA 94720
e-mail: armero@ce.berkeley.edu

Key words: Finite strain multiplicative plasticity, nonlinear dynamics, time-stepping algorithms, energy-momentum schemes.

Summary. *This contribution presents a new time-stepping algorithm for dynamic finite strain plasticity that exhibits the same exact non-negative energy dissipation and momentum conservation of the underlying physical system. In particular, it shows exact energy conservation for elastic steps. These properties rely on a new return mapping algorithm for the integration of the plastic evolution equations. The final scheme is second order accurate in time. General multiplicative models of the $\boldsymbol{F}^e\boldsymbol{F}^p$ type are considered. The new algorithm shows a significantly improved numerical stability when compared with standard schemes like the Newmark trapezoidal rule.*

1 MULTIPLICATIVE FINITE STRAIN PLASTICITY

The deformation $\boldsymbol{\varphi} : \mathcal{B} \times [0,T] \to \mathbb{R}^3$ of a solid $\mathcal{B}$ satisfies the equation of motion

$$\int_{\mathcal{B}} \rho_o \ddot{\boldsymbol{\varphi}} \cdot \delta\boldsymbol{\varphi} \; dV + \int_{\mathcal{B}} \boldsymbol{S} : \boldsymbol{F}^T \mathrm{Grad}\,(\delta\boldsymbol{\varphi}) \; dV = G_{ext}(\boldsymbol{\varphi}, \delta\boldsymbol{\varphi}) \tag{1}$$

for all admissible variations $\delta\boldsymbol{\varphi}$, with a reference density ρ_o, acceleration $\ddot{\boldsymbol{\varphi}}$ and external loading G_{ext}. Of interest here is a finite strain elastoplastic solid characterized by the multiplicative decomposition $\boldsymbol{F} = \boldsymbol{F}^e\boldsymbol{F}^p$ of the deformation gradient $\boldsymbol{F} = \mathrm{Grad}\,\boldsymbol{\varphi}$ and by the second Piola-Kirchhoff stress tensor $\boldsymbol{S}$ given by the hyperelastic relation

$$\bar{\boldsymbol{S}} = 2\,\partial_{\boldsymbol{C}^e} W^e \quad \text{with} \quad \bar{\boldsymbol{S}} = \boldsymbol{F}^p \boldsymbol{S} \boldsymbol{F}^{p^T} \quad \text{and} \quad \boldsymbol{C}^e = \boldsymbol{F}^{e^T}\boldsymbol{F}^e \tag{2}$$

for an elastic potential $W^e(\boldsymbol{C}^e)$. The elastic and plastic parts are given by the evolution equations

$$\left.\begin{array}{c} \boldsymbol{D}^p = \gamma\; \boldsymbol{N}_\phi \;, \quad \boldsymbol{W}^p = \gamma\; \hat{\boldsymbol{M}}_W \;, \quad \dot{\alpha} = \gamma\; n_q \;, \\ \phi(\bar{\boldsymbol{S}}, q; \boldsymbol{C}^e) \leq 0 \;,\; \gamma \geq 0 \;,\; \gamma\phi = 0 \;,\; \gamma\dot{\phi} = 0 \end{array}\right\} \tag{3}$$

with $q = -\partial_\alpha W^h$ for the hardening potential $W^h(\alpha)$, and the plastic rates

$$\boldsymbol{D}^p := \mathrm{symm}\,(\boldsymbol{C}^e\boldsymbol{L}^p) \;, \quad \boldsymbol{W}^p := \mathrm{skew}\,(\boldsymbol{C}^e\boldsymbol{L}^p) \quad \text{for} \quad \boldsymbol{L}^p = \dot{\boldsymbol{F}}^p \boldsymbol{F}^{p^{-1}} \;. \tag{4}$$

A typical choice for the flow vectors in (3) is given by the associated case defined by $\boldsymbol{N}_\phi = \partial_{\bar{\boldsymbol{S}}}\phi$, $\boldsymbol{n}_q = \partial_q \phi$ and vanishing plastic spin $\hat{\boldsymbol{M}}_W = 0$.

A crucial property of the equations summarized above is the energy relation

$$\frac{d}{dt}\Big[\underbrace{\int_{\mathcal{B}}\left[\frac{1}{2}\rho_o\|\dot{\boldsymbol{\varphi}}\|^2 + W^e + W^h\right]\,dV}_{\text{Total energy } H}\Big] = -\underbrace{\int_{\mathcal{B}}\gamma\ \left[\bar{\boldsymbol{S}} : \boldsymbol{N}_\phi + q n_q\right]\,dV}_{\text{Plastic dissipation } \mathcal{D}\geq 0} \leq 0 \tag{5}$$

(assuming no external loading for brevity) with the last inequality obtained by the proper choice of the flow vectors $\boldsymbol{N}_\phi$ and n_q. Similarly, the linear and angular momenta ($\boldsymbol{l} = \int_{\mathcal{B}}\rho_o\dot{\boldsymbol{\varphi}}\,dV$ and $\boldsymbol{j} = \int_{\mathcal{B}}\rho_o\boldsymbol{\varphi}\times\dot{\boldsymbol{\varphi}}\,dV$, respectively) are conserved along the solutions for no external loading.

2 A NEW ENERGY-DISSIPATIVE MOMENTUM-CONSERVING (EDMC) SCHEME

For a given time increment $[t_n, t_{n+1}]$, we consider the discrete equations

$$\boldsymbol{\varphi}_{n+1} - \boldsymbol{\varphi}_n \ = \ \Delta t\ \boldsymbol{v}_{n+\frac{1}{2}} \tag{6}$$

$$\int_{\mathcal{B}}\rho_o\frac{\boldsymbol{v}_{n+1}-\boldsymbol{v}_n}{\Delta t}\cdot\delta\boldsymbol{\varphi}\,dV + \int_{\mathcal{B}}\boldsymbol{S}_*:\boldsymbol{F}^T_{n+\frac{1}{2}}\text{GRAD}\,(\delta\boldsymbol{\varphi})\,dV \ = \ G_{ext}(\boldsymbol{\varphi}_{n+\frac{1}{2}},\delta\boldsymbol{\varphi}) \tag{7}$$

for the mid-point values $(\cdot)_{n+\frac{1}{2}} = [(\cdot)_n + (\cdot)_{n+1}]/2$. A calculation [1] shows that the conservation laws of linear and angular momenta are preserved by the temporal discretization (6)-(7), the latter holding for a symmetric stress approximation $\boldsymbol{S}_*$.

The main goal is the development of a numerical approximation of the plastic evolution equations (3) that preserves the energy evolution equation (5). This is accomplished by

$$\boxed{\left.\begin{array}{l}\frac{1}{2}\left[\boldsymbol{F}^{p^{-T}}_{n+\frac{1}{2}}\Delta\boldsymbol{C}\boldsymbol{F}^{p^{-1}}_{n+\frac{1}{2}} - \Delta\boldsymbol{C}^e\right] = \Delta\gamma\ \boldsymbol{N}_\phi(\bar{\boldsymbol{S}}_*, q_*; \boldsymbol{C}^e_{n+\frac{1}{2}})\\ \text{skew}\left(\boldsymbol{C}^e_{n+\frac{1}{2}}\Delta\boldsymbol{F}^p\boldsymbol{F}^{p^{-1}}_{n+\frac{1}{2}}\right) = \Delta\gamma\ \hat{\boldsymbol{M}}_W(\bar{\boldsymbol{S}}_*, q_*; \boldsymbol{C}^e_{n+\frac{1}{2}})\\ \alpha_{n+1} - \alpha_n = \Delta\gamma\ n_q(\bar{\boldsymbol{S}}_*, q_*; \boldsymbol{C}^e_{n+\frac{1}{2}})\\ \phi(\bar{\boldsymbol{S}}_*, q_*; \boldsymbol{C}^e_{n+\frac{1}{2}}) = 0\end{array}\right\}} \tag{8}$$

for

$$\bar{\boldsymbol{S}}_* = \bar{\boldsymbol{S}}(\boldsymbol{C}^e_{n+\frac{1}{2}}) + 2\frac{W^e_{n+1} - W^e_n - \bar{\boldsymbol{S}}(\boldsymbol{C}^e_{n+\frac{1}{2}}) : \frac{1}{2}\Delta\boldsymbol{C}^e}{\|\boldsymbol{C}^e_{n+1} - \boldsymbol{C}^e_n\|^2}\Delta\boldsymbol{C}^e \quad \text{and} \quad q_* = -\frac{W^h_{n+1} - W^h_n}{\alpha_{n+1} - \alpha_n} \tag{9}$$

recovering $\boldsymbol{S}_* = \boldsymbol{F}^{p^{-1}}_{n+\frac{1}{2}}\bar{\boldsymbol{S}}_*\boldsymbol{F}^{p^{-T}}_{n+\frac{1}{2}}$. Here we have denoted $\Delta(\cdot) = (\cdot)_{n+1} - (\cdot)_n$ and we note again the common case with $\hat{\boldsymbol{M}}_W = 0$. The left-hand-side of $(8)_1$ defines, in particular, a second order approximation of the plastic strain rate $\boldsymbol{D}^p$.

As shown in [1], equations (8)-(9) lead to the discrete energy evolution equation

$$H_{n+1} - H_n = -\int_{\mathcal{B}} \Delta\gamma \ \left[\bar{\boldsymbol{S}}_* : \boldsymbol{N}_\phi + q_* n_q\right] \ dV \leq 0 \tag{10}$$

recovering exactly the a-priori estimate (5). In particular, we obtain a full energy conservation for elastic steps $\Delta\gamma = 0$. We note the crucial aspect of the new algorithm that the stresses appearing in the governing equation (7) satisfy also plastic consistency. Extensions with an additional high-frequency numerical dissipation can be found [1].

Equations (8)-(9) are solved for the plastic variables $\boldsymbol{F}^p_{n+1}$ and α_{n+1} (obtaining the stress variables $\bar{\boldsymbol{S}}_*$ and q_* in the process) with a scheme common to typical return mapping algorithms, that is, an elastic trial state followed by a plastic corrector. The latter consists of two nested Newton loops to enforce the consistency condition and flow rule, respectively. The final scheme leads to an algorithmic consistent tangent in closed-form for the linearization of the global equations (6)-(7). Details can be found in [1].

3 REPRESENTATIVE NUMERICAL SIMULATION

We consider the three-dimensional solid depicted in Figure 1. The solid's constitutive response is given by a finite strain model of J_2-flow theory, based on Mises yield surface and a logarithmic hyperelastic model (Hencky's law) for the elastic response. A more flexible set of parameters is assumed for the arms compared with the central core. The solid is given an initial velocity, leading to the free-flight depicted in Figure 1 in its initial stages. The spatial distribution of the equivalent plastic strain α is also depicted, showing the plasticity developing in the arms for the observed large finite strains.

Figure 2 includes the evolution of the total energy obtained with the new EDMC scheme presented above for different time steps Δt. Plots of the linear and angular momenta (not shown) confirm their conservation for the new EDMC scheme. The dissipation/conservation properties of this scheme are clear: full energy conservation is observed for elastic steps and a strictly positive energy dissipation for plastic steps. These properties hold unconditionally of the time step. This situation is to be contrasted with the solutions obtained by the standard Newmark trapezoidal rule in combination with a now standard exponential return mapping algorithm, as also shown in Figure 2. The lack of energy dissipation/conservation is clear in this case, leading to a blow up of the energy at some stage of the computation resulting in its termination. The improved numerical stability of the new EDMC scheme becomes apparent.

Acknowledgments: We gratefully acknowledge the financial support for this research by the AFOSR under contract no. FA9550-05-1-0117 with UC Berkeley.

REFERENCES

[1] F. Armero. Energy–dissipative momentum–conserving time–stepping algorithms for finite strain multiplicative plasticity. *Comp. Meth. Appl. Mech. Eng.*, to appear,2005.

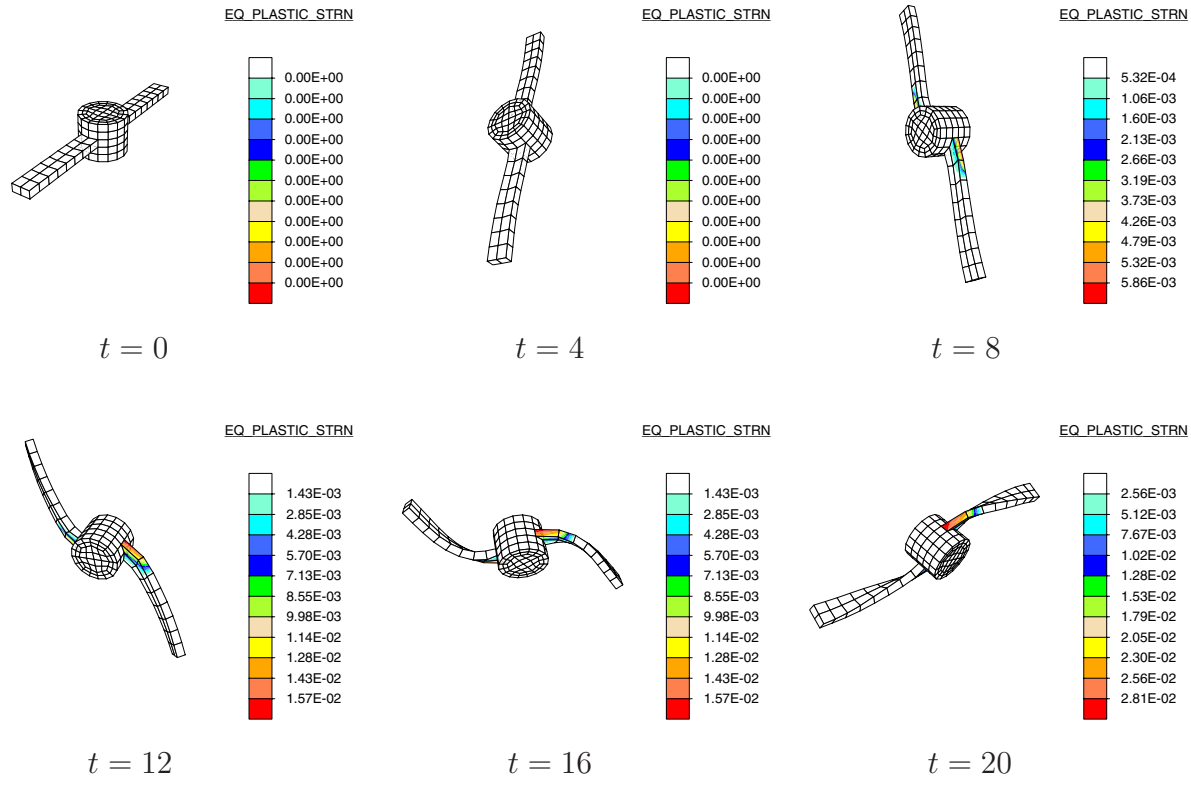

Figure 1: Elastoplastic solid in free flight. Sequence of deformed configurations in the early stages of the motion showing the spatial distribution of the equivalent plastic strain α. Solution obtained with the new EDMC scheme ($\Delta t = 0.5$).

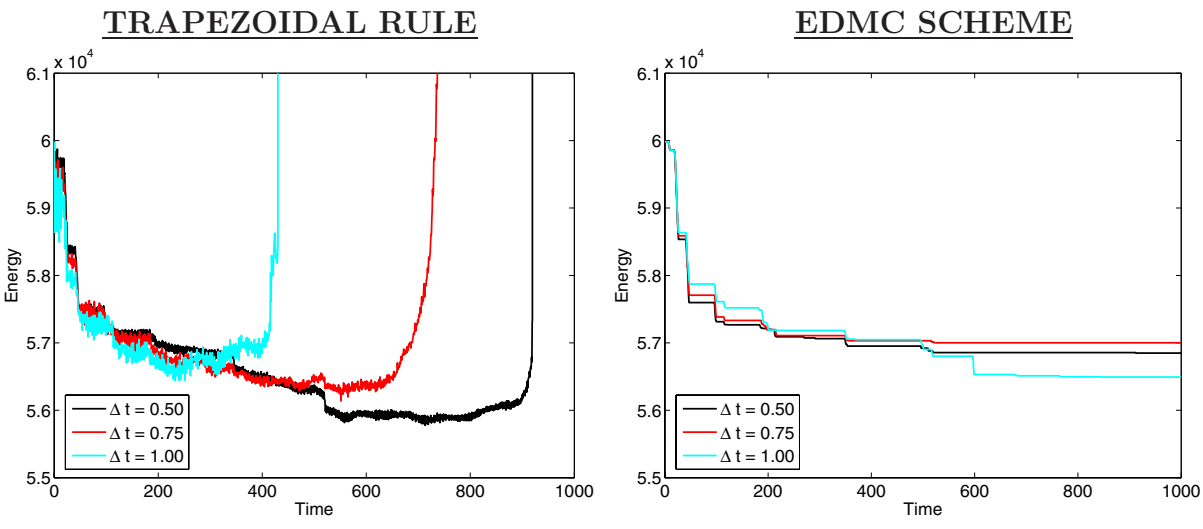

Figure 2: Elastoplastic solid in free flight. Temporal evolutions of the total energy obtained by the Newmark trapezoidal rule (left) and the new EDMC scheme (right) for different time steps.